APPLIED PHYSICS LETTERS 108, 092403 (2016)

Enhanced refrigerant capacity in Gd-Al-Co microwires with a biphase nanocrystalline/amorphous structure

H. X. Shen,[1,2] D. W. Xing,[1] J. L. Sánchez Llamazares,[3] C. F. Sánchez-Valdés,[4]
H. Belliveau,[2] H. Wang,[5] F. X. Qin,[5] Y. F. Liu,[1] J. F. Sun,[1] H. Srikanth,[2] and M. H. Phan[2,a)]
[1]School of Materials Science and Engineering, Harbin Institute of Technology, Harbin 150001, China
[2]Department of Physics, University of South Florida, Tampa, Florida 33620, USA
[3]Instituto Potosino de Investigación Científica y Tecnológica A.C., Camino a la Presa San José 2055 Col. Lomas 4a, San Luis Potosí, S.L.P. 78216, Mexico
[4]Centro de Nanociencias y Nanotecnología, Universidad Nacional Autónoma de México, AP 14, Ensenada 22860, Baja California, Mexico
[5]Institute for Composites Science and Innovation (InCSI), College of Materials Science and Engineering, Zhejiang University, Hangzhou 310027, China

(Received 14 October 2015; accepted 20 February 2016; published online 2 March 2016)

A class of biphase nanocrystalline/amorphous $Gd_{(50+5x)}Al_{(30-5x)}Co_{20}$ ($x=0$, 1, 2) microwires fabricated directly by melt-extraction is reported. High resolution transmission electron microscopy and Fourier function transform based analysis indicate the presence of a volume fraction (~20%) of ~10 nm sized nanocrystallities uniformly embedded in an amorphous matrix. The microwires possess excellent magnetocaloric properties, with large values of the isothermal entropy change ($-\Delta S_M \sim 9.7$ J kg^{-1} K^{-1}), the adiabatic temperature change ($\Delta T_{ad} \sim 5.2$ K), and the refrigerant capacity ($RC \sim 654$ J kg^{-1}) for a field change of 5 T. The addition of Gd significantly alters T_C while preserving large values of the ΔS_M and RC. The nanocrystallites allow for enhanced RC as well as a broader operating temperature span of a magnetic bed for energy-efficient magnetic refrigeration.
 [http://dx.doi.org/10.1063/1.4943137]

Magnetic refrigeration based on the magnetocaloric effect (MCE) of a magnetic solid material is a very promising technology due to its high cooling efficiency, lower energy costs, and environmental affability as compared to conventional gas compression-based refrigeration technology.[1–4] Currently, there is a large amount of research focusing on exploiting magnetic materials with large isothermal magnetic entropy change (ΔS_M) over a broad temperature range, namely, those exhibiting a large refrigerant capacity (RC).[3,4] RC measures the amount of heat that can be transferred between the hot and cold sinks by the magnetic refrigerant in an ideal thermodynamic cycle. The working temperature span of a magnetic refrigerant is given by the temperature difference between T_{hot} and T_{cold} that defines the full-width at half-maximum (FWHM) of the ΔS_M(T) curve, i.e., $\delta T_{FWHM} = T_{hot} - T_{cold}$. A variety of approaches for achieving an increase in RC, such as successive magnetic transitions,[5,6] magnetic field sensitive magnetic phase transitions,[7] and multiple magnetic phase composites,[8,9] have been proposed.

Recently, there has been a growing interest in wire-shaped magnetocaloric materials.[10–17] As compared with their bulk counterparts, the wires with increased surface-to-volume areas allow for a higher heat transfer between the magnetic refrigerant and surrounding liquid. Theoretical studies have revealed that a magnetic bed composed of magnetocaloric wires will yield an optimal device performance.[18,19] In particular, Kuz'min has shown that shaping magnetic refrigerants in the form of spherical or irregular particles is inefficient because of their high energy losses on viscous resistance and demagnetization.[18] Mechanical instability of the refrigerant can result in a significant loss of throughput due to maldistribution of flow. In a detailed analysis, Vuarnoz and Kawanami have theoretically shown that as compared to a magnetic bed made of Gd particles, a bed consisting of Gd wires yields a greater temperature span between its ends, which, in effect, results in a higher cooling efficiency.[19] In this context, our experimental efforts in the development of amorphous melt-extracted Gd-alloy microwires with enhanced RC represent an important task.[11,13,14,16,20] As compared to bulk metallic glass (BMG) and ribbon counterparts, the microwires exhibit larger values of ΔS_M and RC along with their improved mechanical strength. This is due to their shape and inter-wire interaction effects.[11,13] We have shown that the presence of structural disorder significantly broadens the paramagnetic to ferromagnetic (PM-FM) transition and $\Delta S_M(T)$ without significantly altering the nature of the second-order magnetic transition (SOMT) and long-range ferromagnetic order.[20] It is the large magnetic moment of Gd and the presence of the long-range ferromagnetic order that result in the large ΔS_M along with the broadening of the PM-FM transition that contributes to the large RC in the amorphous melt-extracted Gd-alloy microwires. It has recently been reported that the partial nanocrystallizing of an amorphous magnetic material via an appropriate heat treatment will create a biphase nanocrystalline/amorphous structure which significantly improves the RC relative to its amorphous counterpart.[21] This finding has motivated us to exploit Gd-alloy microwires with a biphase nanocrystalline/amorphous structure in order to improve RC.

a)Author to whom correspondence should be addressed. Electronic mail: phanm@usf.edu

In this letter, we report upon an enhanced *RC* in biphase nanocrystalline/amorphous microwires of $Gd_{(50+5x)}Al_{(30-5x)}Co_{20}$ ($x = 0$, 1, 2), which have been directly fabricated by the melt-extraction technique. The *RC* values of the microwires are greater than those of their BMGs and Gd-Al-Co-based ribbons.[22–28] Using these wires, we have proposed a design of a magnetic bed with enhanced *RC* and δT_{FWHM}. Our study paves a pathway for the development of biphase microwires with desirable magnetocaloric properties for active magnetic refrigeration in Micro Electro Mechanical Systems (MEMS) and Nano Electro Mechanical Systems (NEMS).

$Gd_{(50+5x)}Al_{(30-5x)}Co_{20}$ ($x = 0$, 1, 2) microwires with a biphase nanocrystalline/amorphous structure were created directly by adjusting the melt-extraction parameters, details of which have been reported elsewhere.[13] A field-emission scanning electron microscope (SEM-Helios Nanolab600i) at 20 kV was used to observe the micromorphology. X-ray diffraction (XRD, D/max-rb with Cu Kα radiation) was used to examine the phase structure of the microwires. A transmission electron microscope (TEM, Tecnai G2 F30) and a high resolution TEM (HRTEM) were used to take images of the microwires. Selected area electron diffraction (SAED) was also used to analyze the wires. Magnetic measurements were performed using a Magnetic Property Measurement System (MPMS) from Quantum Design. The wire specimens were prepared in the form of a bundle of wires (60 wires) with an average length of ~3 mm. We placed the pre-weighed wires one by one in a sample holder with an inner diameter of 1 mm. Magnetic fields of up to 5 T were applied along the axial direction of the wires. The thermal relaxation method using the heat capacity option of a Physical Property Measurement System (PPMS) Evercool-I platform from Quantum Design was employed to precisely measure $C_p(T, \mu_0 H)$ as a function of temperature (2–160 K) in different fields of $\mu_0 H = 0$, 2, and 5 T.

Figure 1(a) shows an SEM image of the fabricated Gd-Al-Co wires, which possess smooth surfaces with an average diameter of ~30 μm. All the wires display the halo patterns without visible crystalline peaks within the XRD instrument limitation (Fig. 1(b)). However, the TEM and SAED for the $x = 2$ sample show evidence of the presence of a volume fraction (~20%) of nanocrystallities of ~10 nm size embedded in an amorphous matrix. The nanocrystalline area (blue square) and the amorphous matrix (red square) were analyzed by Fourier Function Transform (FFT) and Inverse Fourier Function Transform (IFFT) method (Figs. 1(d) and 1(e)), showing slight variation in the chemical elements. The volume fractions of nanocrystallities for the other wires were also determined to be ~20% as a result of the small compositional variations and the same preparation procedure.

Figure 2 shows the temperature dependence of magnetization (*M-T*) for the wires measured under a field ($\mu_0 H$) of 20 mT. As shown in Fig. 2(a), the *M-T* curves exhibit a broad FM-PM transition around the Curie temperatures (T_C). The values of T_C are determined as the minima of the d*M*/d*T* vs. *T* curves, as displayed in the inset of Fig. 2(a). T_C increases with Gd addition; $T_C = 86$ K, 100 K, and 109 K for $Gd_{50}Al_{30}Co_{20}$, $Gd_{55}Al_{25}Co_{20}$, and $Gd_{60}Al_{20}Co_{20}$, respectively. Hysteresis loops (M-$\mu_0 H$) were measured at 20 K for all the wires and indicate a soft magnetic characteristic (due to the nature of SOMT). This is a desirable quality for active magnetic refrigeration. The saturation magnetization ($M_S \sim 200$ A m^2 kg^{-1}) is large for all the wires and increases with increasing the Gd content as expected (see Fig. 2(b)).

Isothermal magnetization (M-$\mu_0 H$) curves were measured in fields of up to 5 T over a wide temperature range of 20–200 K and have been used to evaluate ΔS_M of the wire samples through the Maxwell's relationship[1]

$$\Delta S_M(T, \mu_0 H) = \mu_0 \int_0^{H_{max}} \left(\frac{\partial M}{\partial T}\right)_H dH, \tag{1}$$

where *M* is the magnetization under a magnetic field $\mu_0 H$, and *S* is the magnetic entropy at a given temperature *T*. Figure 3(a) shows the temperature dependence of ΔS_M for all the wire samples for $\mu_0 \Delta H = 2$ and 5 T. It is clear that the wires exhibit broad ΔS_M (*T*) curves (δT_{FWHM} of ~90 K for $\mu_0 \Delta H = 5$ T), with the largest values of ΔS_M obtained at their T_C temperatures. The maximum value of ΔS_M, denoted as ΔS_M^{max}, is almost unchanged with the addition of Gd (Fig. 3(b)). For $\mu_0 \Delta H = 5$ T, $-\Delta S_M^{max} \cong 10.1$ J kg^{-1} K^{-1} in the $Gd_{50}Al_{30}Co_{20}$ wires, which is almost equal to that of pure Gd (~10.2 J kg^{-1} K^{-1})[4] and is much larger than those of other candidates in the similar temperature range.[22–28]

The increased values of ΔS_M^{max} and δT_{FWHM} (Fig. 3(a)) point to a large *RC* of the microwires. In order to confirm this, the *RC* of the fabricated samples has been determined using the following formula:[29]

$$RC = \int_{T_{cold}}^{T_{hot}} -\Delta S_M(T) dT, \tag{2}$$

where T_{cold} and T_{hot} are the onset and offset temperatures of δT_{FWHM}. Enlarged values of *RC* are obtained for all the samples (Fig. 3(b)). For $Gd_{50}Al_{30}Co_{20}$ wires, *RC* has reached a large value of ~672 J kg^{-1} for $\mu_0 \Delta H = 5$ T. For comparison, the *RC* values of the present microwires and of BMGs and Gd-Al-Co-based amorphous ribbons are plotted in Fig. 3(c).[22–28] The larger values of *RC* in addition to their desirable geometries make the microwires more attractive for applications in magnetic refrigeration. A theoretical study of Franco *et al.* has shown an enhancement of *RC* in biphase magnetic systems as a result of magnetic interactions between the phases.[30] In case of our biphase microwires, magnetic coupling between the nanocrystalline and amorphous phases could result in the broadened SOMTs (Fig. 2(a)) and hence the enhanced *RC* values (Fig. 3(b)).

Due to the lack of specific heat $C_p(T, \mu_0 H)$ measurements on wire-shaped samples, no information on the adiabatic temperature change (ΔT_{ad}) of Gd-based microwires has been reported in previous reports.[11,13,14,16,20] The inset of Fig. 3(d) shows the $C_p(T, \mu_0 H)$ curves of $Gd_{55}Al_{25}Co_{20}$ wires for $\mu_0 H = 0$ and 5 T. The $C_p(T, \mu_0 H)$ curves exhibit the peaks around the T_C, and their λ-like shape is in accordance with the *M-H* data, both of which reveal the SOMT nature of the wires. The ΔT_{ad} of the wires has been calculated by[31]

$$\Delta T_{ad}(\Delta H, T) = [T(S)_{H_1} - T(S)_{H_0}]_S. \tag{3}$$

For $Gd_{55}Al_{25}Co_{20}$ wires, $\Delta T_{ad} \sim 5.2$ K at $\mu_0 \Delta H = 5$ T at its T_C of 100 K. This value of ΔT_{ad} is about half of pure Gd

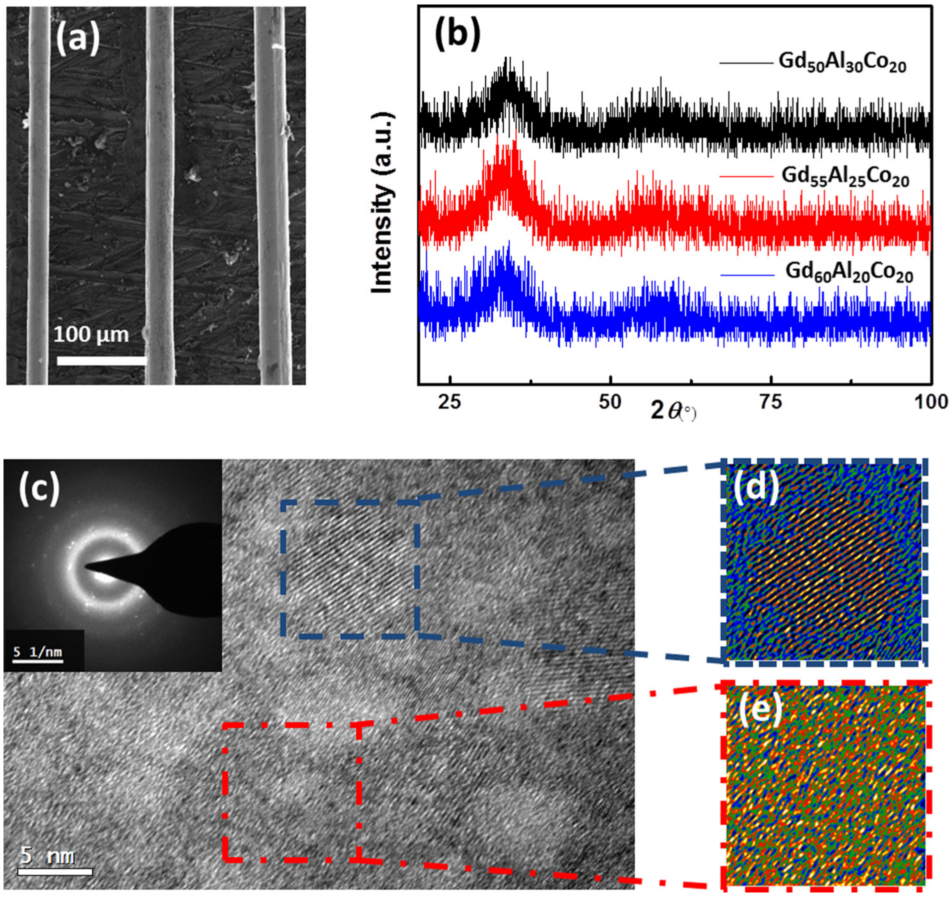

FIG. 1. (a) SEM and (b) XRD patterns of $Gd_{(50+5x)}Al_{(30-5x)}$ Co_{20} ($x=0$, 1, 2) microwires. (c) TEM and SAED (inset of c) images of the $x=2$ sample. In (d) and (e), the corresponding Fourier transforms of the nanocrystalline regions and the amorphous matrix are shown.

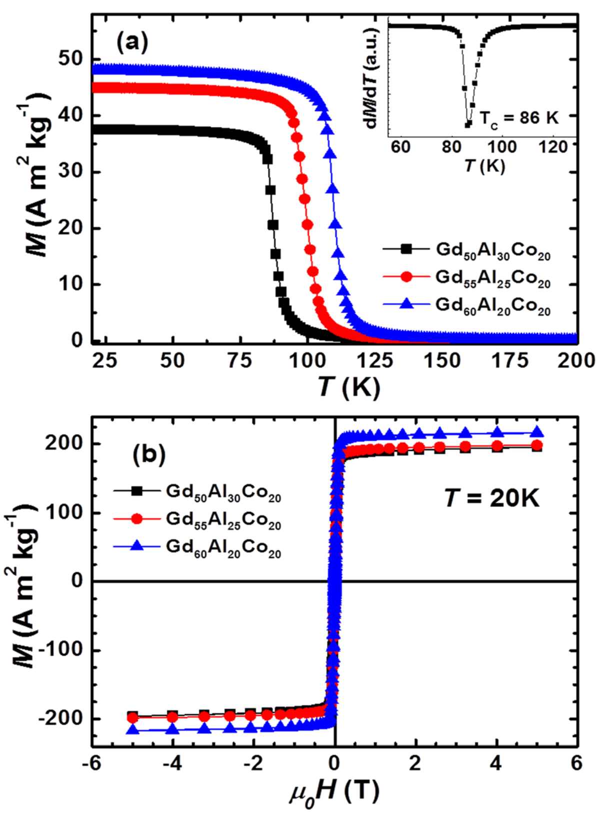

FIG. 2. (a) M vs. T curves under a field of 20 mT of $Gd_{(50+5x)}Al_{(30-5x)}Co_{20}$ ($x=0$, 1, 2) microwires. Inset of Fig. 2(a) shows the dM/dT vs. T curve of the $x=0$ sample. (b) The hysteresis loops (M-μ_0H) of the wires measured at 20 K.

($\sim$11 K at $\mu_0\Delta H = 5$ T at $T_C = 294$ K).[32] However, the $\Delta T_{ad} \cong 1.8$ obtained at $\mu_0\Delta H = 2$ T for $Gd_{55}Al_{25}Co_{20}$ wires is about 8 times larger than that reported for NiMnGa glass-coated microwires ($\Delta T_{ad} \cong 0.22$ K at $\mu_0\Delta H = 1.8$ T at $T_C = 320$ K). This would provide the impetus needed to develop Gd-based microwires for active magnetic refrigeration.

From an engineering perspective, a magnetic bed containing a stack of magnetocaloric wires will yield a better device performance as compared to that made of magnetocaloric particles.[18,19] The bundle of closely packed cylindrical wires, as illustrated in Fig. 4(a) (denoted as Specimen-1), is desirable for use in active magnetic refrigerators. This is because of their high mechanical stability and low porosity.[18] Considering two wires that possess similar values of ΔS_M but different values of T_C (namely, $Gd_{50}Al_{30}Co_{20}$ wires with $-\Delta S_M = 10.09$ J kg^{-1} K^{-1} and $T_C = 86$ K; $Gd_{60}Al_{20}Co_{20}$ with $-\Delta S_M = 10.11$ J kg^{-1} K^{-1} and $T_C = 109$ K), we design an alternative magnetic bed (denoted as Specimen-2) composed of these wires that are arranged in a one-by-one fashion as illustrated in Fig. 4(b). Using the experimental MCE data of $Gd_{50}Al_{30}Co_{20}$ and $Gd_{60}Al_{20}Co_{20}$ (denoted as Wire A and Wire B, respectively) and considering their equal weight fractions, we have calculated the temperature dependence of $-\Delta S_M$ for Specimen-2 following the relation: $-\Delta S_{M(S\text{-}2)} = \alpha\Delta S_{M(A)} + \beta\Delta S_{M(B)}$, where α and β are the relative weight fractions of the two wires (here $\alpha = \beta = 50\%$).[33] We have plotted in Fig. 4(c) the $-\Delta S_M$ (T) curves for Wire A, Wire B, and Specimen-2 for $\mu_0\Delta H = 5$ T. It can be observed that although the $-\Delta S_M^{max}$ of Specimen-2 ($\sim$9 J kg^{-1} K^{-1} for $\mu_0\Delta H = 5$ T) is slightly smaller than those of both Wire A and Wire B ($\sim$10.09 and

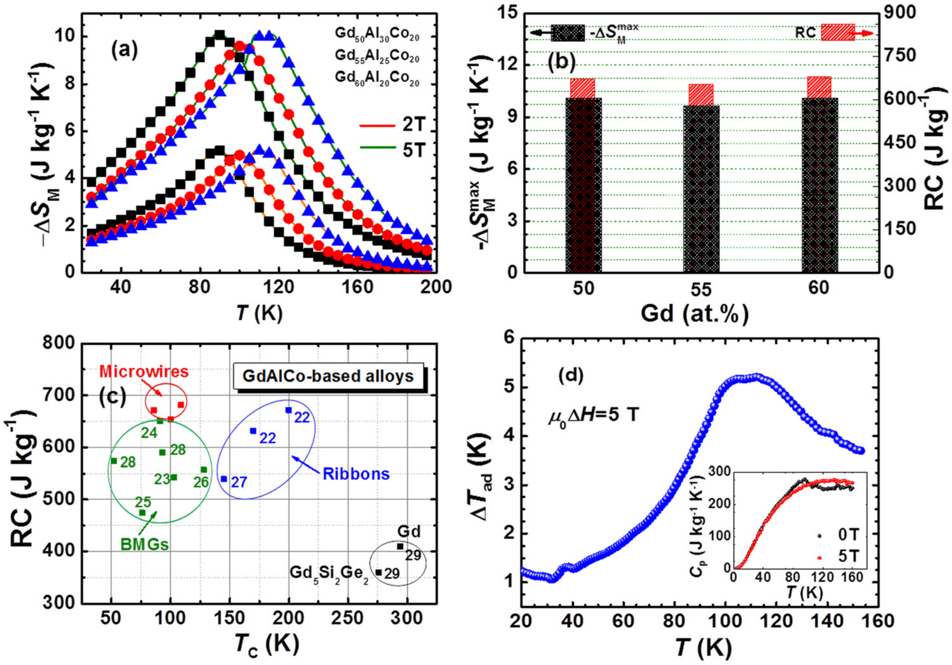

FIG. 3. (a) $-\Delta S_M(T)$ curves of $Gd_{(50+5x)}Al_{(30\text{-}5x)}Co_{20}$ ($x=0$, 1, 2) wires for $\mu_0\Delta H=2$ and 5 T; (b) the $-\Delta S_M{}^{max}$ values and *RC* values of these wires at $\mu_0\Delta H=5$ T. (c) *RC* with respect to T_C of the present wires in comparison with Gd-Al-Co-based BMGs and amorphous ribbons reported in the literature. (d) Temperature dependence of the adiabatic temperature change (ΔT_{ad}) at $\mu_0\Delta H=5$ T for $Gd_{55}Al_{25}Co_{20}$ wires; the inset of (d) shows the temperature-dependent heat capacity $C_P(T)$ measured at $\mu_0H=0$ and 5 T.

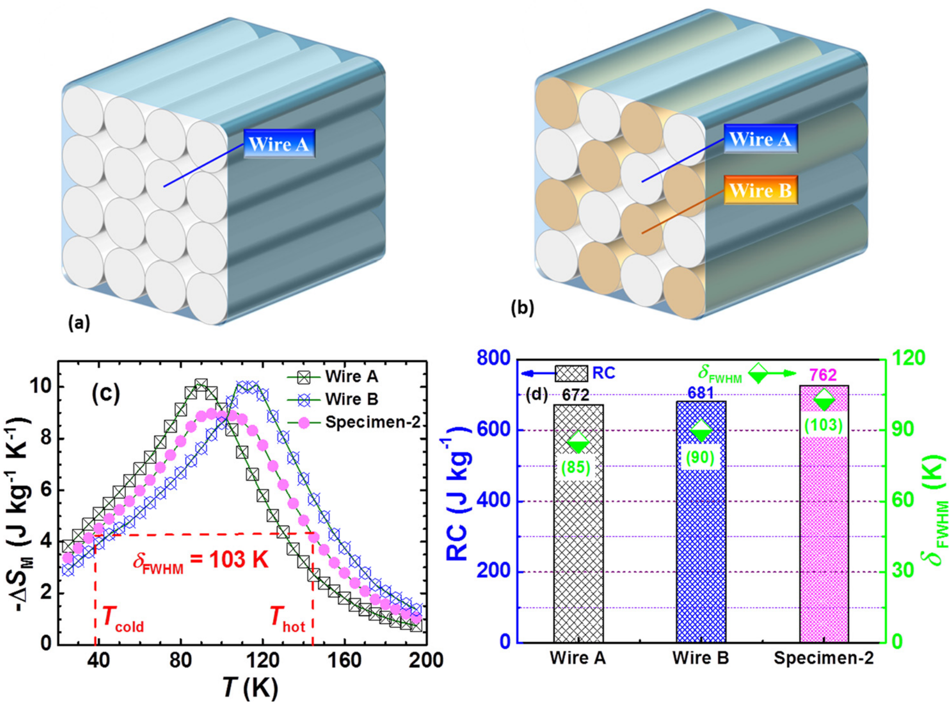

FIG. 4. (a) A magnetic regenerator bed made of closely packed cylindrical wires that have the same ΔS_M and T_C; (b) a magnetic regenerator bed made of closely packed cylindrical wires that have similar values of ΔS_M but different values of T_C; (c) $-\Delta S_M$ (*T*) plots for Wire A, Wire B, and Specimen-2 for $\mu_0\Delta H=5$ T; (d) the corresponding values of *RC* and δT_{FWHM} for the samples at $\mu_0H=5$ T.

10.11 J kg^{-1} K^{-1} for $\mu_0\Delta H=5$ T, respectively), the $-\Delta S_M$ (*T*) curve is much broader for Specimen-2. The δT_{FWHM} of the $-\Delta S_M$ (*T*) curve for Specimen-2 is ~103 K, which is about 20% and 14% larger than those for Wire A (~86 K) and for Wire B (~90 K), respectively. As a result of this, the *RC* value of Specimen-2 (~726 J kg^{-1}) is greater than those of Wire A (~672 J kg^{-1}) and Wire B (~681 J kg^{-1}). The table-like MCE shape (i.e., the relatively constant ΔS_M with temperature) is also observed for Specimen-2, which is beneficial for Ericsson-cycle based magnetic refrigerators.[1,4]

In summary, we have shown the excellent magnetocaloric properties in $Gd_{(50+5x)}Al_{(30-5x)}Co_{20}$ ($x=0$, 1, 2) microwires with a biphase nanocrystalline/amorphous structure. We have also demonstrated an effective approach for enhancing both the *RC* and the operating temperature span of a magnetic bed by using wires that have similar values of the magnetic entropy change but different Curie temperatures. The present microwires are attractive candidates for their use in active magnetic refrigerators operating in the liquid nitrogen temperature range.

The work was partially supported by the National Natural Science Foundation of China (NSFC) No. 51371067 (Sample fabrication and structural chracterization). H. X. Shen acknowledges the fellowship from China Scholarships Council (CSC, No. 201406120138). H.S. and M.H.P. acknowledge the support from the U.S. Department of Energy, Office of Basic Energy Sciences, Division of Materials Sciences and Engineering under Award No. DE-FG02-07ER 46438 (magnetocaloric studies). J. L. Sánchez Llamazares acknowledges the support received from Laboratorio Nacional de Investigaciones en Nanociencias y Nanotecnología (LINAN, IPICyT, Specific heat measurements). C. F. Sánchez-Valdés wishes to thank CTIC-UNAM for supporting his current postdoctoral position at CNyN-UNAM. F.X.Q. acknowledges the financial support of NSFC No. 51501162 (TEM analysis). The authors thank Dr. Chen Peng of Heilongjiang University for some magnetic measurements.

[1]V. Franco, J. S. Blázquez, B. Ingale, and A. Conde, Annu. Rev. Mater. Res. **42**, 305 (2012).
[2]D. Eriksen, K. Engelbrecht, C. R. H. Bahl, R. Bjørk, K. K. Nielsen, A. R. Insinga, and N. Pryds, Int. J. Refrig. **58**, 14 (2015).
[3]E. Brück, J. Phys. D: Appl. Phys. **38**, R381 (2005).
[4]K. A. Gschneidner, Jr., V. K. Pecharsky, and A. O. Tsokol, Rep. Prog. Phys. **68**, 1479 (2005).
[5]G. X. Li, J. L. Wang, Z. X. Cheng, Q. Y. Ren, C. S. Fang, and S. H. Dou, Appl. Phys. Lett. **106**, 182405 (2015).
[6]L. W. Li, T. Namiki, D. X. Huo, Z. H. Qian, and K. Nishimura, Appl. Phys. Lett. **103**, 222405 (2013).
[7]L. W. Li, O. Niehaus, M. Kersting, and R. Pöttgen, Appl. Phys. Lett. **104**, 092416 (2014).
[8]P. J. Ibarra-Gaytán, J. L. Sánchez Llamazares, P. Álvarez-Alonso, C. F. Sánchez-Valdés, P. Gorria, and J. A. Blanco, J. Appl. Phys. **117**, 17C116 (2015).
[9]I. G. de Oliveira, P. J. von Ranke, and E. P. Nóbrega, J. Magn. Magn. Mater. **261**, 112 (2003).
[10]M. I. Ilyn, V. Zhukova, J. D. Santos, M. L. Sánchez, V. M. Prida, B. Hernando, V. Larin, J. González, A. M. Tishin, and A. Zhukov, Phys. Status Solidi A **205**, 1378 (2008).
[11]N. S. Bingham, H. Wang, F. Qin, H. X. Peng, J. F. Sun, V. Franco, H. Srikanth, and M. H. Phan, Appl. Phys. Lett. **101**, 102407 (2012).
[12]A. Zhukov, V. Rodionova, M. Ilyn, A. M. Aliev, R. Varga, S. Michalik, A. Aronin, G. Abrosimova, A. Kiselev, M. Ipatov, and V. Zhukova, J. Alloys Compd. **575**, 73 (2013).
[13]F. X. Qin, N. S. Bingham, H. Wang, H. X. Peng, J. F. Sun, V. Franco, S. C. Yu, H. Srikanth, and M. H. Phan, Acta Mater. **61**, 1284 (2013).
[14]H. Shen, H. Wang, J. Liu, D. Xing, F. Qin, F. Cao, D. Chen, Y. Liu, and J. Sun, J. Alloys Compd. **603**, 167 (2014).
[15]J. D. Dong, A. R. Yan, and J. Liu, J. Magn. Magn. Mater. **357**, 73 (2014).
[16]Y. F. Liu, X. Zhang, D. W. Xing, H. X. Shen, D. M. Chen, J. S. Liu, and J. F. Sun, J. Alloys Compd. **616**, 184 (2014).
[17]X. X. Zhang, M. F. Qian, Z. Zhang, L. S. Wei, L. Geng, and J. F. Sun, Appl. Phys. Lett. **108**, 052401 (2016).
[18]M. D. Kuzmin, Appl. Phys. Lett. **90**, 251916 (2007).
[19]D. Vuarnoz and T. Kawanami, Appl. Therm. Eng. **37**, 388 (2012).
[20]A. Biswas, T. L. Phan, N. H. Dan, S. C. Yu, M. H. Phan, and H. Srikanth, J. Appl. Phys. **115**, 17A907 (2014).
[21]C. F. Sánchez-Valdes, P. J. Ibarra-Gaytan, J. L. Sánchez Llamazares, M. Avalos-Borja, P. Álvarez-Alonso, P. Gorria, and J. A. Blanco, Appl. Phys. Lett. **104**, 212401 (2014).
[22]B. Schwarz, B. Podmilsak, N. Mattern, and J. Eckert, J. Magn. Magn. Mater. **322**, 2298 (2010).
[23]J. Du, Q. Zheng, Y. B. Li, Q. Zhang, D. Li, and Z. D. Zhang, J. Appl. Phys. **103**, 023918 (2008).
[24]Q. Luo and W. H. Wang, J. Alloys Compd. **495**, 209 (2010).
[25]L. Liang, X. Hui, and G. L. Chen, Mater. Sci. Eng., B **147**, 13 (2008).
[26]W. H. Wang, Adv. Mater. **21**, 4524 (2009).
[27]B. Schwarz, N. Mattern, J. D. Moore, K. P. Skokov, O. Gutfleisch, and J. Eckert, J. Magn. Magn. Mater. **323**, 1782 (2011).
[28]Q. Luo, D. Q. Zhao, M. X. Pan, and W. H. Wang, Appl. Phys. Lett. **89**, 081914 (2006).
[29]K. A. Gschneidner and V. K. Pecharsky, Annu. Rev. Mater. Sci. **30**, 387 (2000).
[30]C. Romero-Muñiz, V. Franco, and A. Conde, Appl. Phys. Lett. **102**, 082402 (2013).
[31]L. W. Li, Y. Yuan, Y. K. Zhang, T. Namiki, K. Nishimura, R. Pöttgen, and S. Q. Zhou, Appl. Phys. Lett. **107**, 132401 (2015).
[32]S. Yu. Dan'kov, A. M. Tishin, V. K. Pecharsky, and K. A. Gschneidner, Jr., Phys. Rev. B **57**, 3478 (1998).
[33]P. Álvarez, P. Gorria, J. L. Sánchez Llamazares, and J. A. Blanco, J. Alloys Compd. **568**, 98 (2013).